Mucus-Inspired Supramolecular Adhesives with Oil-Regulated Molecular Configurations and Long-Lasting Antibacterial Properties

Wenqing He; Zhaoyue Wang; Changshun Hou; Xin Huang; Bo Yi; Yuhe Yang; Wenrui Zheng; Xin Zhao; Xi Yao*

ABSTRACT: Inspired by mucus, which provides an ideal supramolecular model and whose fluid-like (viscous) and solid-like (elastic) behaviors can be adjusted to meet different physiological requirements, we report oil-regulated supramolecular adhesives by the co-assembly of polyurea oligomers and carvacrol oils. The adhesive is crosslinked by weak but abundant hydrogen bonds, which can be regulated by the incorporated carvacrol oils through the competition of intermolecular hydrogen bonds, presenting a unique set of mucus-mimicking features including oil-regulated mechanics, processability, reusable adhesivity, and extreme longevity in both air and water. Owing to the intrinsic bactericidal effect of the carvacrol oils, the developed adhesives can serve as potent antibacterial coatings with both rapid contact killing (99.9% killing within 15 min) and long-term controlled release abilities (up to 70 days), enabling versatile antibacterial applications in diverse conditions. We envision that these adhesives will be useful in buildings and architectures, community and public facilities, food storage and packaging technologies, functional textiles, and practical biomedical fields.

KEYWORDS: bioinspired, supramolecular adhesives, oligomer, hydrogen bonds, antibacterial

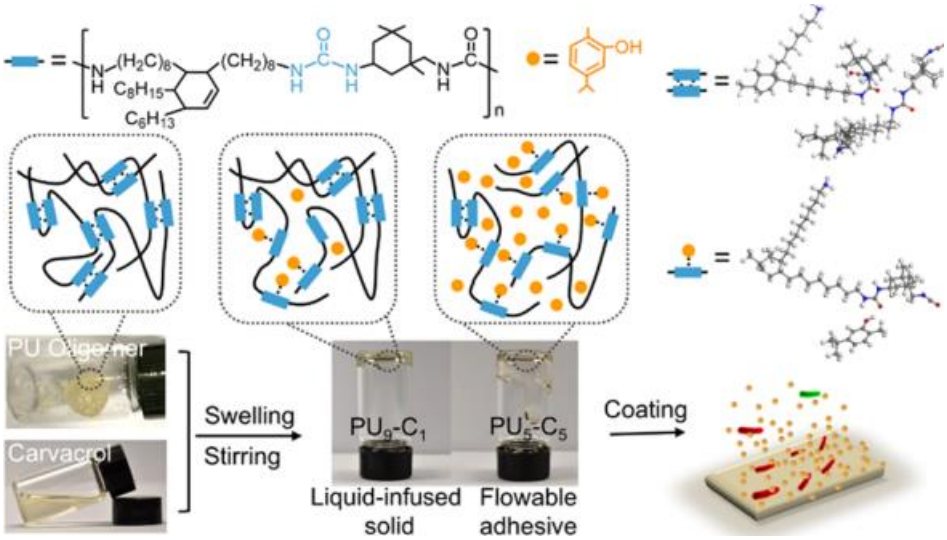

Introduction

Indiscriminate and overuse of antibiotics in animals, humans, and environment led to the evolution of bacteria with antimicrobial resistance (AMR). (1) An environment-friendly strategy to combat AMR is to utilize biogenic agents, such as antimicrobial peptides, (2,3) quorum-sensing inhibitors, (4) and bacteriolytic enzymes. (5) Nevertheless, their applications have been limited due to poor proteolytic stability and relatively high cost. Plant-derived essential oils (EOs), which protect plants against pathogenic infection, have emerged as “green” biogenic bactericides because of their excellent biocompatibility, low cost, and potent antibacterial activities. (6,7) They exhibit broad-

spectrum bactericidal properties with multiple antibacterial mechanisms so that it is difficult for bacteria to develop AMR. (8) However, poor solubility of EOs in aqueous solutions has seriously limited their practical uses. (9) A straightforward strategy is to increase the aqueous solubility through colloidal delivery carriers stabilized by surfactants, nanoparticles, (10) or polymers. (11,12) Although these methods could facilitate the dispersion of EOs in aqueous mediums, (13,14) they still suffer from poor stability and low loading capacity. Furthermore, as these EO-encapsulating materials are designed for function in aqueous mediums, they are not suitable for a variety of applications, for example, as antimicrobial coatings, adhesives, and additives for persistent contact killing and quick disinfection in both dispersed (planktonic) and biofilm settings. (15,16).

Nature is abundant in liquid-infused materials, which present a feature of liquid-dependent functionality. (17−20) Mucus is a complex adherent secretion that lines the epithelial surfaces of various animals (Scheme 1), which provides an ideal model as a viscoelastic supramolecular network mainly composed of glycoproteins and water through weak but abundant hydrogen bonding interactions. (21) It provides a barrier against pathogens with a unique set of physicochemical and mechanical properties, where fluid-like (viscous) and solid-like (elastic) behaviors can be adjusted to meet different physiological requirements through the manipulation of water secretion. Besides, the supramolecular network of mucus can incorporate antimicrobial peptides or lysozymes that can help the disinfection of trapped pathogens. (22) To date, the supramolecular assembly has been extensively used not only to incorporate functional elements (23−31) such as photosensitizers, (32) antibiotics, (33) and nanoparticles (34,35) for antibacterial applications but also to adjust molecular configurations and mechanical properties. Recently, the supramolecular assembly strategy based on water-participant hydrogen bonding has been adopted to tune the material mechanics and adhesion properties. (36,37) Although the individual features aforementioned have been realized, respectively, it is a lack of strategy that enables the harvest of all of the features into a single material without compromising each other. Inspired by the supramolecular design of mucus, we herein proposed a new EO participating supramolecular assembly strategy toward the development of antibacterial adhesives with long-term stability, EO-regulated mechanics, and high antibacterial efficiency without developing AMR to adapt to various application requirements.

Scheme 1. Schematic Showing the Versatile Location of Mucus[a]

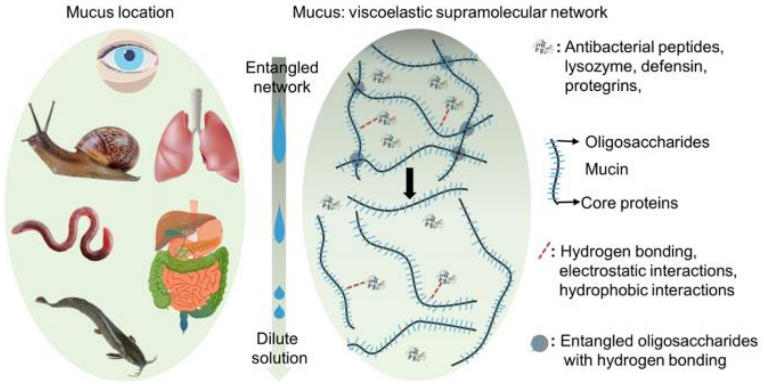

[a]It is an ideal model for supramolecular design with multiple interactions including hydrogen bonding, electrostatic interactions, etc. The defensive compounds such as antibacterial peptides, lysozyme, and defensin are well immobilized within the mucus and perform functions (e.g., antibacterial, bacterial/particulate adhesion, and clearance) according to different physiological requirements.

Specifically, the supramolecular adhesive was prepared by the co-assembly of polyurea (PU) oligomers and carvacrol oils (one kind of EO molecules) based on hydrogen bonding. The PU oligomers, molecules with high-density urea groups, were synthesized through a one-pot reaction

with industrial chemicals and then assembled with carvacrol oils by simply mixing (swelling or stirring) PU oligomers (via the urea group) and carvacrol oils (via the hydroxyl group), resulting in the supramolecular polyurea–carvacrol (PU–C) adhesive. Through this process, intermolecular hydrogen bonds that crosslinked PU oligomers were partially replaced by hydrogen bonds between PU and carvacrol, which are more energy-favorite. Similar to water molecules in mucus, the carvacrol molecules induce and mediate the molecular configurations, mechanics, and antibacterial properties in the PU–C adhesive, endowing the supramolecular system with a set of mucus-mimicking features including processability, damage-tolerance, transparency, reusable adhesivity, tunable mechanical property, and a persistent antibacterial feature. To the best of our knowledge, no other supramolecular polymeric material with all of these features in a single polymeric system has been designed.

Results and Discussion

The synthesis route of PU oligomers involved the one-pot reaction of Priamine 1074 and isophorone diisocyanate (IPDI) at room temperature (Figure S1a), resulting in nonsticky glass-like PU oligomers with a molecular weight around 5051 (Figures 1a and S1b). According to its powder X-ray diffraction (PXRD) pattern (Figure S1c), the PU oligomers were amorphous. After stirring the PU oligomers in carvacrol oil for 24 h (Movie S1), the mixture became homogeneous. The resultant PUm–Cn (m/n, w/w) materials manifested good transparency at different carvacrol concentrations (Figure S2). The attenuated total reflectance-Fourier-transform infrared spectroscopy (ATR-FTIR) and 1H NMR measurements were adopted to monitor the synthesis process and to reveal the molecular interaction between the PU oligomers and the carvacrol molecules (Figures S1d, S3, and S4). With the increased addition of carvacrol oil, one representative IR peak related to hydrogen-bonded OH shifted from 3312 to 3392 cm–1 (Figure 1b), indicating the existence of hydrogen bonding between carvacrol molecules (via the hydroxyl group) and the PU oligomers (via the urea group). (38−40) This hydrogen bonding can also be confirmed with the 1H NMR peak of the OH group shifting from 4.65 to 4.82 ppm when comparing carvacrol and PU9–C1 (Figure S4). Further simulations and calculations based on density functional theory (DFT) confirmed that the averaged hydrogen bond strength (EHB) between carvacrol molecules and PU oligomer units was stronger than that between two PU oligomer units (Figures 1a and S5), revealing the dissociation tendency of PU oligomer stacks and the reassembly between PU oligomers and carvacrol molecules. Furthermore, with the increased amount of carvacrol oil in the PUm–Cn materials (e.g., from PU to PU5–C5), the measured glass transition temperature (Tg) decreased from 49 to −30 °C (Figure 1c), indicating the improved mobility of oligomers, which could be ascribed to the dissociation of the hydrogen-bonded PU stacks. Thermogravimetric analysis (TGA) showed that the offset temperature of carvacrol decomposition (Toffset) in the PUm–Cn materials increased with the increasing carvacrol addition, revealing the abundant interactions between the PU oligomers and the carvacrol molecules (Figure S6). These results proved that the carvacrol molecules in the molecular configurations of the PUm–Cn materials serve as a hydrogen bond competitor, contribute to the dissociation of PU stacks, and regulate the mobility of the PU oligomers in the PUm–Cn materials.

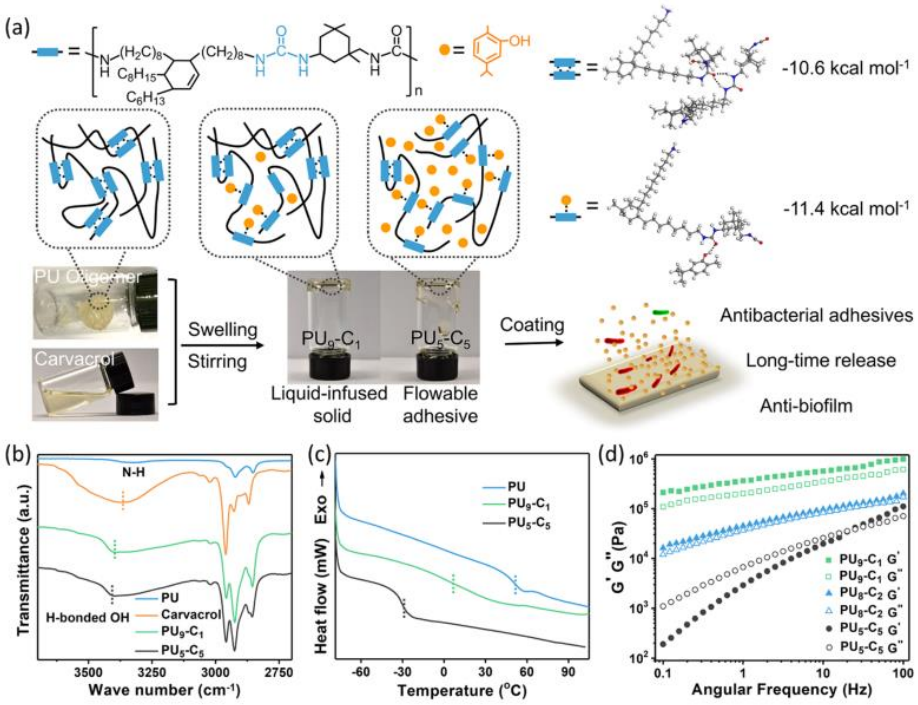

Figure 1. Preparation and application of supramolecular adhesive based on hydrogen bond. (a) PU oligomers and carvacrol oil are assembled together with hydrogen bond interactions. Relatively stronger hydrogen bonds between the PU and the carvacrol molecules (-11.4 kcal mol^{-1}) gradually replace the hydrogen bonds among PU (-10.6 kcal mol^{-1}) with the increase of carvacrol molecules. The gray, red, blue, and white spheres in the atomic structures correspond to carbon, oxygen, nitrogen, and hydrogen atoms, respectively. (b) ATR-IR spectra showing the red shift of the peak from 3312 to 3392 cm^{-1}, corresponding to the hydrogen-bonded OH groups. (c) Addition of carvacrol oil decreases the T_g of the supramolecular polymer. (d) Dynamic frequency sweep rheological experiments demonstrating the elastic response of PU_9-C_1 and viscoelastic behaviors of PU_5-C_5.

Such oil-regulated molecular configurations would further affect the bulk properties of the PUm–Cn materials. To demonstrate that the carvacrol oil uptake is responsible for the drastic property changes, PUm–Cn samples with different carvacrol content were prepared. As expected, the addition of carvacrol oil significantly altered the physical state and mechanical properties of the samples. For example, PU9–C1 (9:1, w/w) exhibited shape persistence in typical upturn tests, making it more like a liquid-infused solid, while PU5–C5 (5:5, w/w) presented as a viscous adhesive that can deform slowly on an inverted tube. The fluidic nature of PU5–C5 makes it damage-tolerant and easy to process in both air and in aqueous mediums such as Luria–Bertani (LB) broth (Figure S7), while the solid-like PU9–C1 showed a conditioned damage-healing behavior after thermal treatment (Figure S8). These results confirmed that the carvacrol uptake dramatically changed the macroscopic appearance, viscosity, and damage-tolerant ability of the PU–C materials.

Dynamic frequency sweep rheological experiments were used to quantitatively evaluate the mechanical properties of the PU–C materials. Figures 1d and S9 show the change of the storage moduli (G′) and loss moduli (G″) of PUm–Cn (m/n = 9:1, 8:2, 5:5, 4:6, 3:7, 2:8) as a function of angular frequency at a fixed strain (1%). Both the G′ values and the G″ values decreased almost 8 and 6 orders of magnitude, respectively, with the increase of the carvacrol content from 10 to 80 wt %, demonstrating that the representative carvacrol oil could regulate mechanical properties of materials. For example, PU9–C1 showed the elastic response of the material as its G′ was higher than G″. The crossover point of G′ and G″ appearing in the sample PU5–C5 confirmed its nature of flowable adhesive because of the viscous behavior on relatively lower frequencies and elastic behavior on higher frequencies. When the carvacrol content was further increased to 60% or above, the PU–C materials responded as viscoelastic liquids, for which the G′ values were lower than the G″ values over the entire range of the tested frequencies (36) (Figure S9). Such oil-regulated

mechanical property together with the ease of formulation of different PU–C materials facilitate their broad applications in practical scenarios.

The addition of carvacrol oil also endows easy processability of the resulting PU–C materials. Taking PU5–C5 as an example, bundles of parallel fibers could be pulled when the material was first deposited between two glass slides that were subsequently pulled apart, which is also evidence for the high molecular weight of the supramolecular polymeric structures (Figure 2a,b). The fibers' surface is smooth, with the diameter down to 5 μm (Figure 2c, upper). They could be rolled up or deposited on different substrates (Movie S2), staying intact for over 6 months without any obvious cracking (Figure 2c, bottom). The PU5–C5 also can be injected in air or underwater for the continuous production of fibers and fiber stacks (Figures 2c and S10).

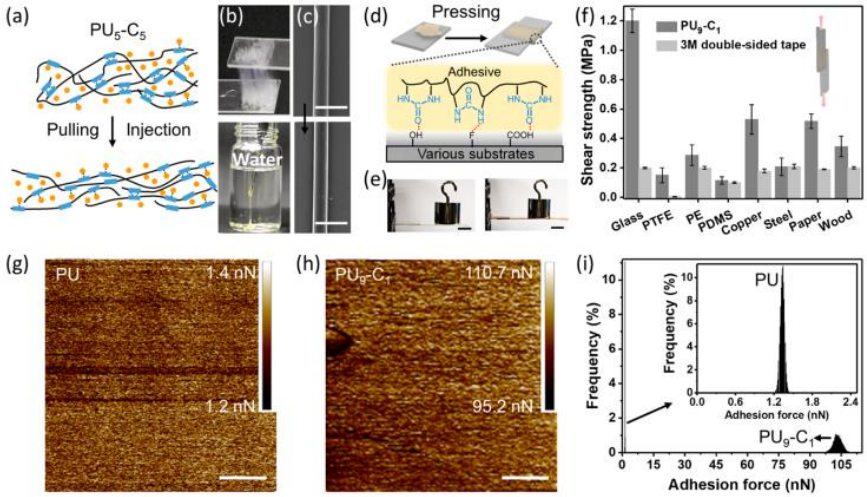

Figure 2. (a) Schematic showing the good processability of PU_5-C_5. (b) PU_5-C_5 microfibers can be made by pulling in air (upper part) or injecting underwater (bottom part, coumarin 6 was added to PU_5-C_5 to make it visible underwater). (c) Scanning electron microscopy (SEM) images revealing that the prepared microfiber can maintain its morphology for 6 months and the diameter maintains around 5 μm (up: original microfiber, bottom: microfiber after exposure in air for 6 months). (d) Schematic revealing the adhesion procedure and its mechanism. (e) Images showing adhesive behavior of PU_9-C_1 materials sandwiched between glass and copper plates. A weight of 500 g was put on one side of the adhered plate. (f) Comparison of shear strengths between PU_9-C_1 and commercial 3M double-sided tape on eight types of substrates. (g, h) Atomic force microscopy (AFM) adhesion force images ($5 \times 5\ \mu m^2$) of the PU and PU_9-C_1. (i) Distributions of adhesion forces measured between the bare AFM tip and the PU (see inset figure) and PU_9-C_1. The average adhesion force of the PU_9-C_1 is 101.2 nN, which is much higher than that of PU oligomers (1.3 nN), indicating the oil-regulated adhesion property. Scale bar: (c) 10 μm, (e) 2 cm, and (g, h) 1 μm.

Although the PU–C materials are composed of a large number of oils, they are not slippery like many other oil-infused materials. (17−20,41) Instead, they are excellent adhesives with special oil-regulated properties. Owing to the abundant acylamino groups and phenolic hydroxyl groups in the PU–C materials, they can adhere to various substrates with the hydrogen bond mediated interfacial binding (38,39,42−44) (Figure 2d–f). In a typical experiment, PU9–C1 film with ca. 50 μm thickness was thermal cast onto different substrates followed by a tensile shear strength test. In comparison to the commercial 3M double-sided tape, PU9–C1 displayed much better adhesion ability on different tested surfaces including metals, plastics, and even poly(tetrafluoroethylene) (PTFE) (Figure 2f). For example, the shear strength of 1.20 MPa is measured on a hydrophilic glass slide, 0.12 MPa for poly(dimethylsiloxane) (PDMS) films, and 0.15 MPa for Teflon. The adhesion properties could be ascribed to the processability and gap-filling capability of PU9–C1 in the thermal casting process, as well as the adhesive force formed by the high-density H-bonds between the acylamino groups of the PU–C and the hydroxyl groups of hydrophilic surfaces or the fluorine groups of hydrophobic Teflon surfaces. After the tensile tests, the ruptured adhesive on the separated sample substrates, for example, copper foils, could rebind under compression at 4 MPa and room temperature or hot-pressing at 1 MPa and 80 °C (Figure S11) due to the supramolecular nature of

the adhesive and the reconfiguration of the PU oligomers and the carvacrol molecules. Even after 10 cycles of rupture and rebinding, no substantial decrease was observed in the measured shear strength of the adhesive, indicating valuable and promising reusability. (36) Moreover, AFM adhesion force analyses were performed (Figure 2g–i), and the average adhesion force of PU9–C1 is 101.2 nN, which is almost 80 times that of PU oligomers (1.3 nN), proving the oil-regulated adhesion property. Due to universal adhesivity and good processability, the PU–C materials can be applied as a versatile platform for coating applications.

Meanwhile, the adhesives have intrinsic antibacterial properties due to the addition of carvacrol oils. Carvacrol oil is a nonvolatile organic liquid with a boiling point at 237 °C in ambient condition, and its solubility in water is very low (8.3 mM), making it favorable for long-term usage in both air and underwater. Further longevity tests demonstrated that the PU–C materials showed prolonged retention and slow-releasing profiles of the incorporated carvacrol oils in both air and underwater. In the air, the evaporation rates of carvacrol oil in the PU–C materials were significantly lower than that of raw carvacrol oil, which should be contributed by both the shielding effect of the supramolecular network and the dissociation retardancy of hydrogen bonding between the PU oligomers and the carvacrol oils (Figure 3a). Specifically, the measured evaporation rates (mass) for carvacrol oil in PU9–C1 and PU5–C5 are ~0.02 and ~0.11% day–1, which are ~31- and ~6-fold lower than those of the raw carvacrol oils, ~0.62% day–1, respectively (Figure 3b). While in typical cumulative releasing tests, in which the adhesives were put in a water bath that was refreshed daily, the supramolecular adhesive PU5–C5 with a higher carvacrol oil loading amount than PU9–C1 could sustain a long-time release for up to 70 days (Figures 3c and S12).

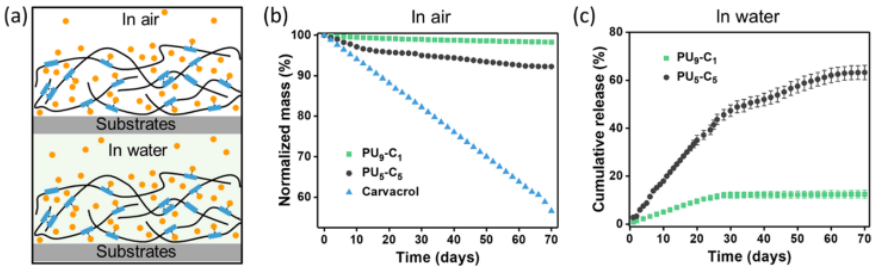

Figure 3. (a) Schematic representing the longevity of PU−C materials when exposed to air and long-time release property when exposed to water. (b) Plot showing the mass change of the PU−C adhesives in air for a 70-day period. (c) Cumulative release curve showing that the supramolecular adhesive PU_5-C_5 can sustain long-time release for up to 70 days in water.

Surfaces and coatings with antibacterial properties have the potential to decorate public facilities and clinical devices to block bacterial transmission. As a proof-of-demonstration, the live/dead bacterial viability assay was performed on Gram-positive bacteria (S. aureus, B. subtilis) and Gram-negative bacteria (E. coli, P. aeruginosa) after contacting with glass slides (control group) or PU9–C1-coated glass slides for 15 min (Figure 4a,b). A double staining kit containing SYTO 9, which stains live cells (green), and propidium iodide (PI), which binds to the DNA and thus stains dead cells (red), was used for the simultaneous staining of the living and the dead cells. Almost all intact bacteria fluoresced green, while almost all bacteria contacted with the coated glasses fluoresced red after contact for 15 min, demonstrating excellent and rapid antibacterial activities of the PU9–C1 coating. To further elucidate the antibacterial mechanism of the PU9–C1, we investigated the morphological changes of bacteria cells before and after treatment with PU9–C1-coated glass. For the control group, Bacillus subtilis, Escherichia coli, and Pseudomonas aeruginosa showed characteristic rod shapes with smooth surfaces, and Staphylococcus aureus displayed sphere-like shapes (inset figures in Figure 4a). However, the cell walls and membranes of the

bacteria became rough and were seriously disrupted after contacting with coated glass (inset figures in Figure 4b). A disk diffusion test was then adopted to evaluate the antibacterial properties of PU–C materials with different carvacrol oil content (Figure S13). As expected, the results showed that the diameter of the inhibition zone increased (from 11.8 to 18.1 mm for S. aureus and from 7.4 to 14 mm for E. coli) as the carvacrol oil content increased from 10 to 70 wt %.

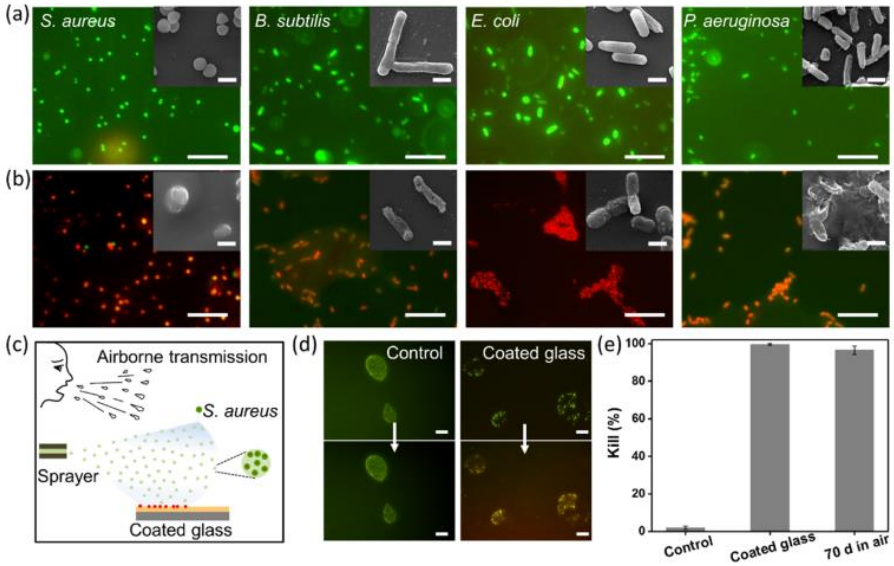

Figure 4. Antibacterial effect of supramolecular adhesive $PU_9{-}C_1$. Live/dead viability assay of *S. aureus*, *B. subtilis*, *E. coli*, and *P. aeruginosa* before (a) and after (b) contact with $PU_9{-}C_1$ for 15 min (inset SEM images showing the morphology of the corresponding bacterial cells). (c) Schematic showing the airborne transmission process by coughing and the experimental setup to mimic this process. Microdroplets containing *S. aureus* are sprayed onto the coated substrate. (d) *In situ* observation of *S. aureus* in microdroplets by live/dead viability assay when contacted with bare glass (left) and coated glass (right) before and after 15 min (white arrows meant that 15 min elapsed). (e) Quantitative study on the killing efficiency of original $PU_9{-}C_1$ and $PU_9{-}C_1$ after exposure in air for 70 days. Scale bar: (a, b) 10 μm, inset figure 1 μm, and (d) 50 μm.

Airborne droplets (>5 μm), aerosols (<5 μm), and particles generated in violent respiratory events, such as coughing and sneezing, can serve as the media for bacterial transmission and virus spread by floating in air and contaminating public facilities. (16,45) Therefore, rapid disinfection of bacteria on microdroplet contaminated surfaces is a useful and economic strategy to control the spread of many infectious diseases. To mimic the sneezing/coughing process, microdroplets containing S. aureus (106 CFU/mL) were generated and sprayed onto the PU9–C1-coated glass (Figure 4c). The live/dead bacterial viability assay was applied to S. aureus wrapped by microdroplets. In situ observation under fluorescence microscope indicated that most bacteria were dead within 15 min (Figure 4d). Quantitative analysis revealed that the killing efficiency of the PU9–C1 coatings was >99.9% for fresh samples and could be maintained above 95% after exposure in air for 70 days (Figure 4e), indicating long-term retention of the carvacrol oil in the coating and the longevity of the PU9–C1 material as an antibacterial coating for the prevention of airborne transmitted bacteria/pathogens.

The PU–C materials could also be directly used underwater for bactericidal application due to the ease-of-processability and substrate binding ability, while the pure carvacrol oil cannot directly perform functions in the aqueous medium due to the water immiscibility and poor water solubility. As discussed previously, the viscoelastic PU–C materials (e.g., PU5–C5) could be injected/painted on surfaces and sustain long-time release in aqueous mediums. They thus can be used as a paint or coating on submerged objects (e.g., plate, tubing, and mesh) for water disinfection with a synergistic killing effect: bacteria become dead immediately after direct contact with the PU–C-coated area due to the high concentration of carvacrol molecules on the localized region, whereas the planktonic

bacteria can be killed by the released carvacrol molecules in the medium (Figure 5a). In a typical experiment where 2 mL of water was deposited into a well of a 24-well plate, in which the bottom was coated with 60 mg of PU–C materials, the diffused carvacrol oil can reach the minimal inhibitory concentration (MIC) for both S. aureus and E. coli within 6 h when PU5–C5 is used (Figure 5b,c). Subsequently, the sample-dependent antimicrobial test of the PU–C materials was done by the addition of bacterial suspension instead of water to the coated 24-well plate (Figures 5d and S14). With the increased oil percentage in PU–C materials, the concentrations of S. aureus and E. coli decreased accordingly, after a 2 h treatment and testing by the colony-forming unit (CFU) method. The time-dependent antimicrobial effect showed that the concentrations of both S. aureus and E. coli decreased more than 6 orders of magnitude within 6 h when the well bottoms were coated with PU5–C5 (Figures 5e and S14). In a cumulative release test where the bacterial medium was refreshed daily, the killing efficiency of the PU5–C5 coated sample maintained above 90% after 60 days and >82% after 70 days, respectively (Figure 5f). Such a long-term bactericidal effect is an exception compared to current commercially available products. (46,47).

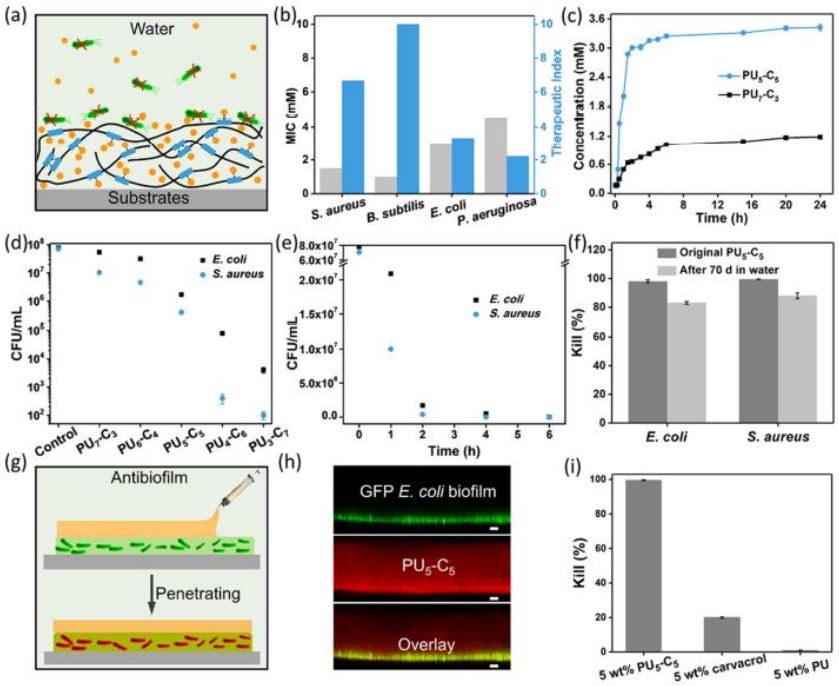

Figure 5. Supramolecular adhesive PU_5−C_5 can be used to disinfect water and treat biofilm. (a) Schematic showing the synergistic killing effect of antibacterial supramolecular coatings. (b) Minimal inhibitory concentration and therapeutic index (HC50/MIC) of carvacrol oil for *S. aureus, B. subtilis, E. coli,* and *P. aeruginosa*. (c) Release profile of carvacrol oil in a coated well with 2 mL of water. (d) Concentration-dependent antimicrobial effects of PU−C materials against Gram-positive (*S. aureus*) and Gram-negative (*E. coli*) bacteria after a 2 h treatment. (e) Time-dependent antimicrobial effects of PU_5−C_5 materials against *S. aureus* and *E. coli* bacteria. (f) Killing efficiency of original PU_5−C_5 and PU_5−C_5 after cumulative release test in bacterial suspension for 70 days on *E. coli* and *S. aureus* after a 2 h treatment. (g) Schematic showing that the supramolecular adhesive PU_5−C_5 can penetrate the biofilm. (h) Confocal image stacks and penetration profile of *E. coli* biofilm after 1 h treatment with PU_5−C_5. (i) Killing efficiency of PU_5−C_5, carvacrol oil, and PU on 1-day-old *E. coli* biofilm after a 1 h treatment. Scale bar: (h) 20 μm. Standard error bars are too small to be visible for some points at the plotted scales.

Extracellular polymeric substances (EPS) in biofilm serve as a potent barrier against therapeutic treatments. (48) The viscoelastic nature of the PU–C adhesives enables the direct casting or painting onto regions with biofilms, which can facilitate the diffusion and penetration of carvacrol oils into the biofilms. The ability of PU5–C5 materials to penetrate biofilms was monitored using confocal microscopy. Biofilms formed by green fluorescent protein (GFP)-expressing E. coli were prepared on glass slides after culturing for 24 h in LB broth, which were further treated by depositing PU5–C5 labeled by Nile red dyes. As shown in Figure 5g,h, fluorescently labeled PU5–C5 materials readily penetrated and dispersed throughout the biofilms in 1 h. The quantitative analysis (Figure

S15) demonstrated that PU5–C5 penetrated the biofilm efficiently, reaching the enclosed bacteria deep within the matrix of the film. Moreover, in a 1 h treatment, the penetration of carvacrol oil released from PU5–C5 adhesive is able to kill over 99.5% bacteria in the biofilm, which is more potent than the diffusive manner presented previously. The PU5–C5 adhesive demonstrated a distinctively enhanced killing efficiency compared with the individual components (Figure 5i), indicating that the combination of PU and carvacrol oil to produce PU–C adhesive is crucial for maximum therapeutic efficiency.

Ideal antibacterial materials should not only exhibit excellent antibacterial effect but also have negligible toxicity to mammalian cells. (49) To assess the cytocompatibility of the PU oligomers and carvacrol oils, a cell viability test was conducted on these materials. Almost all of the Chinese hamster ovary fibroblasts cells (CHO-K1) were alive and exhibited normal shapes, revealing the satisfying biocompatibility of oligomers and carvacrol oils (Figure S16a–e). We also adopt a hemolysis activity assay to further evaluate the biocompatibility of different concentrations of the carvacrol oils on red blood cells (Figure S16f). When incubating with red blood cells, the carvacrol oil remained nonhemolytic up to a measured concentration of around 4 mM. Moreover, the 50% hemolytic concentration (HC50) was calculated to be 10 mM, which was 2–10 times higher than the MIC values of different bacterial strains, indicating an acceptable selectivity for bacterial cells over human red blood cells (Figure 5b). (46,50−52)

Conclusions

In summary, a mucus-inspired supramolecular adhesive has been prepared through the EO-regulated hydrogen bonding in a simple mixing and formulation method. The developed materials exhibited a couple of mucus-mimicking properties including room-temperature processability, transparency, reusable adhesivity, and more importantly, liquid-regulated mechanical properties and bactericidal ability. With the oil-regulated features, these materials can be applied as versatile antibacterial coatings with adjustable mechanics, substrate binding, high killing efficiency, and prolonged longevity in various working conditions. Considering the aforementioned properties and the ease of manufacture, such oil-infused adhesives hold the potential to serve as versatile antibacterial platforms in various industrial-scale applications, including building and packaging technologies, textile and fabrics, pharmaceuticals, and other biomedical fields. Furthermore, our design can be extended to develop versatile oil-infused biomaterials with on-demand functional integrity based on rational combinations of polymer oligomers and functional liquids, which provides a new and efficient approach for material development. We envision that not only polymer oligomers with various noncovalent interaction motifs and backbones could be introduced but also other molecules with biological activities can be involved to provide complementary means in the fight against bacteria/viruses or other applications. Specifically, a recent study showed that some respiratory viruses such as HCoV 19 can remain viable for multiple hours in aerosols and up to days on different surfaces including metals and plastics. (53) While the current strategy to control surface contamination is regular disinfection by alcohol or bleach solution, which is time-consuming and not sustainable, our strategy of mucus-inspired coating might directly address the issues of virus/pathogen-contained aerosol.

Experimental Section

Materials

Dimer diamines (Priamine 1074) were purchased from CRODA Coatings & Polymers. Isophorone diisocyanate (IPDI), coumarin 6 (98%), and Nile red, which stained PU5–C5 for confocal observation, were purchased from Sigma-Aldrich.

Synthesis of Polyurea (PU) Oligomers and the Preparation of Supramolecular Adhesive PUm–Cn

Polyurea was synthesized by the reaction between Priamine 1074 and IPDI (Figure S1a). Typically, 1 g of Priamine 1074 was dissolved in 20 mL of dichloromethane (DCM) and then poured into a three-necked round bottom flask with a condenser, dropping funnel, and a magnetic stirrer bar. IPDI (0.42 g) was dissolved in 20 mL of dichloromethane (DCM) and the solution was added dropwise in 30 min. The mixture was stirred for another 2 h. The reaction was monitored by ATR-FTIR. The supramolecular adhesives PUm–Cn were prepared simply by swelling and stirring with polyurea and carvacrol. The mass ratio of polyurea/carvacrol was variable (9/1–2/8), thus the content of carvacrol was 10, 20, 30, 50, 70, and 80 wt %, respectively.

Characterization

Thermogravimetric analysis (TGA) of the supramolecular adhesives PUm–Cn was carried out on TG 209F1 Libra, NETZSCH with a heating rate of 10 °C min–1. The glass transition temperature (Tg) of PUm–Cn was measured by a differential scanning calorimeter (DSC Q20, TA Instruments) with a heating rate of 10 °C min–1 from −80 to 100 °C. The hydrogen bond between carvacrol and polyurea oligomer was confirmed by ATR-FTIR and 1H NMR tests. Optical transparency was characterized using a UV–visible light spectrophotometer (Shimadzu 1700) with a wavelength ranging from 300 to 800 nm. Dynamic frequency sweep rheological experiments were carried out in the linear viscoelastic regime using a rotational rheometer (Kinexus lab+, Malvern). The strain amplitude was at 1.0%. The atomic force microscopy (AFM) measurements were conducted on Bruker Dimension Icon in the PeakForce tapping mode. The mass loss of pure carvacrol and PUm–Cn was monitored by a high-resolution balance (Mettler Toledo AT460 DeltaRange analytical balance) with a sensitivity of 0.1 mg. The evaporation data were measured for 70 consecutive days in an open area under room conditions.

DFT Calculations of Carvacrol–Polyurea Oligomer Interaction Models

The geometric optimization and frequency calculation of the molecules are carried out at the B3LYP/6–31G* level. The energy of the hydrogen bond in complexes 1, 2, and 3 (Figure S3) is calculated at the B97D4/6-311+G** level. All calculations were performed using the Gaussian 095 software.

Tensile Shear Strength Measurements of PU9–C1 Adhesive Coating to Substrates

PU9–C1 was used as the adhesive and deposited onto a substrate. The deposition area was fixed as 2.5 × 2.0 cm2. After the deposition, another substrate was used to sandwich the deposited adhesive. To homogenously cast the PU9–C1 adhesive material between the two substrates, the substrate–sample–substrate sandwich was hot-pressed at 80 °C for 10 min, then cooled to room temperature before testing. The shear strength experiments were performed on an HY-0580 tension machine (HENGYI Company). The two substrates were adhered between the two fixtures in a vertical direction. The strain rate was 5 mm min–1, and the data were recorded in real time.

Antimicrobial Tests

For contact killing tests, four types of bacteria were adopted as models to test the antibacterial effect, including Gram-positive S. aureus and B. subtilis and Gram-negative E. coli and P. aeruginosa. The SYTO 9/PI Double Stain Kit was used in the live/dead bacterial assay. The bacteria were allowed to grow in the LB broth for 16 h to reach the midlog phase, and then the diluted bacterial suspension

(104–105/mL) was dropped onto an uncoated glass and a glass coated with PU9–C1. The bacteria were observed by an Ni-E upright fluorescence microscope after contact for 15 min. The bacterial morphology on the above glasses was further confirmed by means of a scanning electron microscope (SEM). (20) The microdroplets containing bacteria were generated and sprayed as described in the previous literature. (16) As for the disc diffusion method test, supramolecular adhesives with various percentages of carvacrol were coated on the round shape glass cover of a 6 mm diameter. A bacterial solution of McFarland 0.5 was swabbed uniformly across a culture plate. The glass cover with the coating was then placed on the surface of the LB agar. Then, the LB agar plate was incubated at 37 °C for 16 h, and the inhibition zone was recorded using a camera.

Analysis of Carvacrol Release Rates and Antibacterial Effects in Aqueous Media

The bottoms (the area of the bottom: 190 mm2) of the 24-well plate were overcoated with 60 mg of PUm–Cn materials. Water (2 mL) was added into the coated well and the release of carvacrol underwater was monitored by a UV–vis double-beam spectrophotometer (Hitachi, UH5300). The planktonic bacteria-killing efficiency in the LB broth upon the 24-well plate coated with different PUm–Cn was measured by CFU counting. Specifically, the bottoms of the 24-well plate were overcoated with 60 mg of PUm–Cn. LB broth (2 mL) with known bacterial concentrations was deposited in the coated well. After 2 h, the killing effect could be detected with the CFU method. We could also figure out the influence of treatment time on the killing of bacteria by taking a sample from the same well to carry out the CFU method after a different time period.

PU5–C5 Penetration into Biofilms

The effective treatment of biofilms requires the penetration of antimicrobial agents into the film. We next probed the ability of PU5–C5 to penetrate into biofilms. Nile red-dyed PU5–C5 was used to track their delivery into biofilms formed by green fluorescent protein (GFP)-expressing E. coli. GFP-expressing E. coli (2 mL, ∼107 mL–1) was added to each well of the 12-well microplate. The LB broth without bacteria was used as a negative control. The plates were incubated at room temperature for 24 h. Then, 5 wt % PU5–C5, PU, and carvacrol were incubated with the biofilms for 1 h. Biofilms were washed with phosphate-buffered saline (PBS) three times, and the viability was determined using an Alamar Blue assay. (12)

Live/Dead Cell Viability Assay of CHO-K1 Fibroblasts

CHO-K1 cells were incubated in bare 96-well plates and PU9–C1-coated 96-well plates for 48 h. CHO-K1 cells (5 × 103) were seeded per well in a 96-well plate with 200 μL of DMEM and 10% FBS. After incubating for 48 h, 0.5 μL of 1 mg mL–1 calcein AM (Life technology) and 0.5 μL of 1 mg mL–1 propidium iodide (PI) (Life technology) were added to each well to stain the cells. After incubation at 37 °C for 15 min, the cells became visible under a Ti-E inverted microscope. The intracellular esterases in live cells could convert the calcein AM into a green-fluorescent calcein, where the live cells displayed green fluorescence. PI is not permeant to live cells. Therefore, PI was only bound to DNA in dead cells. The green fluorescence of calcein was excited by a 488 nm laser and measured at 510–600 nm. The red fluorescence of PI was recorded at 650–705 nm with the excitation of a 633 nm laser.

Hemolytic Activity Assay

This assay was conducted according to the literature. (54) Carvacrol was incubated with human red blood cells (RBCs), and its HC50 was calculated. HC50 is defined as the concentration that causes 50% hemolysis of RBCs. First, carvacrol at concentrations from 1 to 6 mM was placed in a 96-well plate. Then, 50 μL of erythrocyte suspension (5% v/v in PBS) was added to 50 μL of carvacrol

solution in each well, with PBS as the negative control and 1% Triton X-100 as the positive control. After incubation for 1 h at 37 °C, the plate was centrifuged at 1500 g for 10 min, and 50 μL of the supernatant was transferred to a new 96-well plate containing 50 μL of PBS in each well. The absorbance was measured at 404 nm. The hemolytic activity was calculated as follows

$$\text{hemolysis}\ (\%) = (A - A_0)/(A_{100} - A_0) \times 100\% \quad (1)$$

where A, A0, and A100 represent the absorbance of carvacrol and the negative and positive controls, respectively.

Minimum Inhibitory Concentrations (MICs)

MIC test was performed according to the literature. (55,56)S. aureus, B. subtilis, and E. coli, P. aeruginosa were cultured and then diluted to 1 × 105 CFU/mL in fresh LB broth. Carvacrol solution (100 μL) in LB broth at concentrations ranging from 0 to 20 mM was added to 96-well plates, and then 100 μL of the bacterial suspension was added into each well. The mixtures were incubated at 37 °C for 16 h. Then, the absorbance of 600 nm of the mixture was recorded with a microreader.

$$\text{the inhibitory index}\ (\%) = (A - A_{\text{blank}})/(A_0 - A_{\text{blank}}) \times 100\% \quad (2)$$

where A represents the absorbance of the test, Ablank represents the absorbance of 200 μL of LB broth, and A0 represents the absorbance of the mixture of the 0 mM carvacrol.

Acknowledgments

W.H., Z.W., and C.H. contributed equally to this work. This work was supported by the Research Grant Council of Hong Kong (Grant Nos. 11274616 and 15202119), City University of Hong Kong (Nos. 7005109 and 7004816), The Hong Kong Polytechnic University (1-ZVPC), and Shenzhen Basic Research Program (JCYJ20180307123925200).

References

This article references 56 other publications.

1 O'Connell, K. M. G.; Hodgkinson, J. T.; Sore, H. F.; Welch, M.; Salmond, G. P. C.; Spring, D. R. Combating Multidrug-Resistant Bacteria: Current Strategies for the Discovery of Novel Antibacterials. Angew. Chem., Int. Ed. 2013, 52, 10706– 10733, DOI: 10.1002/anie.201209979

2 Schnaider, L.; Brahmachari, S.; Schmidt, N. W.; Mensa, B.; Shaham-Niv, S.; Bychenko, D.; Adler-Abramovich, L.; Shimon, L. J. W.; Kolusheva, S.; DeGrado, W. F.; Gazit, E. Self-assembling Dipeptide Antibacterial Nanostructures with Membrane Disrupting Activity. Nat. Commun. 2017, 8, 1365 DOI: 10.1038/s41467-017-01447-x .

3 Zasloff, M. Antimicrobial Peptides of Multicellular Organisms. Nature 2002, 415, 389, DOI: 10.1038/415389a .

4 Kratochvil, M. J.; Welsh, M. A.; Manna, U.; Ortiz, B. J.; Blackwell, H. E.; Lynn, D. M. Slippery Liquid-Infused Porous Surfaces that Prevent Bacterial Surface Fouling and Inhibit Virulence Phenotypes in Surrounding Planktonic Cells. ACS Infect. Dis. 2016, 2, 509– 517, DOI: 10.1021/acsinfecdis.6b00065

5 Glinel, K.; Thebault, P.; Humblot, V.; Pradier, C. M.; Jouenne, T. Antibacterial Surfaces Developed from Bio-inspired Approaches. Acta Biomater. 2012, 8, 1670– 1684, DOI: 10.1016/j.actbio.2012.01.011 .
6 Donsì, F.; Ferrari, G. Essential Oil Nanoemulsions as Antimicrobial Agents in Food. J. Biotechnol. 2016, 233, 106– 120, DOI: 10.1016/j.jbiotec.2016.07.005 .
7 Atarés, L.; Chiralt, A. Essential Oils as Additives in Biodegradable Films and Coatings for Active Food Packaging. Trends Food Sci. Technol. 2016, 48, 51– 62, DOI: 10.1016/j.tifs.2015.12.001 .
8 Lambert, R. J.; Skandamis, P. N.; Coote, P. J.; Nychas, G. J. A Study of the Minimum Inhibitory Concentration and Mode of Action of Oregano Essential Oil, Thymol and Carvacrol. J. Appl. Microbiol. 2001, 91, 453– 462, DOI: 10.1046/j.1365-2672.2001.01428.x .
9 Turek, C.; Stintzing, F. C. Stability of Essential Oils: A Review. Compr. Rev. Food Sci. Food Saf. 2013, 12, 40– 53, DOI: 10.1111/1541-4337.12006 .
10 Duncan, B.; Li, X.; Landis, R. F.; Kim, S. T.; Gupta, A.; Wang, L.-S.; Ramanathan, R.; Tang, R.; Boerth, J. A.; Rotello, V. M. Nanoparticle-Stabilized Capsules for the Treatment of Bacterial Biofilms. ACS Nano 2015, 9, 7775– 7782, DOI: 10.1021/acsnano.5b01696 .
11 Landis, R. F.; Gupta, A.; Lee, Y.-W.; Wang, L.-S.; Golba, B.; Couillaud, B.; Ridolfo, R.; Das, R.; Rotello, V. M. Cross-Linked Polymer-Stabilized Nanocomposites for the Treatment of Bacterial Biofilms. ACS Nano 2017, 11, 946– 952, DOI: 10.1021/acsnano.6b07537 .
12 Landis, R. F.; Li, C.-H.; Gupta, A.; Lee, Y.-W.; Yazdani, M.; Ngernyuang, N.; Altinbasak, I.; Mansoor, S.; Khichi, M. A. S.; Sanyal, A.; Rotello, V. M. Biodegradable Nanocomposite Antimicrobials for the Eradication of Multidrug-Resistant Bacterial Biofilms without Accumulated Resistance. J. Am. Chem. Soc. 2018, 140, 6176– 6182, DOI: 10.1021/jacs.8b03575 .
13 Yuan, G.; Chen, X.; Li, D. Chitosan films and coatings containing essential oils: The antioxidant and antimicrobial activity, and application in food systems. Food Res. Int. 2016, 89, 117– 128, DOI: 10.1016/j.foodres.2016.10.004 .
14 Ramos, M.; Beltrán, A.; Peltzer, M.; Valente, A. J. M.; Garrigós, M. dC. Release and Antioxidant Activity of Carvacrol and Thymol from Polypropylene Active Packaging Films. LWT - Food Sci. Technol. 2014, 58, 470– 477, DOI: 10.1016/j.lwt.2014.04.019 .
15 Stilianakis, N. I.; Drossinos, Y. Dynamics of Infectious Disease Transmission by Inhalable Respiratory Droplets. J. R. Soc. Interface 2010, 7, 1355– 1366, DOI: 10.1098/rsif.2010.0026 .
16 Jiang, J.; Zhang, H.; He, W.; Li, T.; Li, H.; Liu, P.; Liu, M.; Wang, Z.; Wang, Z.; Yao, X. Adhesion of Microdroplets on Water-Repellent Surfaces toward the Prevention of Surface Fouling and Pathogen Spreading by Respiratory Droplets. ACS Appl. Mater. Interfaces 2017, 9, 6599– 6608, DOI: 10.1021/acsami.6b15213 .
17 Wong, T.-S.; Kang, S. H.; Tang, S. K. Y.; Smythe, E. J.; Hatton, B. D.; Grinthal, A.; Aizenberg, J. Bioinspired Self-repairing Slippery Surfaces with Pressure-stable Omniphobicity. Nature 2011, 477, 443– 447, DOI: 10.1038/nature10447 .
18 Yao, X.; Hu, Y.; Grinthal, A.; Wong, T.-S.; Mahadevan, L.; Aizenberg, J. Adaptive Fluid-infused Porous Films with Tunable Transparency and Wettability. Nat. Mater. 2013, 12, 529– 534, DOI: 10.1038/nmat3598 .
19 He, W.; Liu, P.; Zhang, J.; Yao, X. Emerging Applications of Bioinspired Slippery Surfaces in Biomedical Fields. Chem. - Eur. J. 2018, 24, 14864– 14877, DOI: 10.1002/chem.201801368 .
20 He, W.; Liu, P.; Jiang, J.; Liu, M.; Li, H.; Zhang, J.; Luo, Y.; Cheung, H.-Y.; Yao, X. Development of Multifunctional Liquid-infused Materials by Printing Assisted Functionalization on Porous

Nanocomposites. J. Mater. Chem. A 2018, 6, 4199– 4208, DOI: 10.1039/C7TA10780C .
21 Bansil, R.; Turner, B. S. The Biology of Mucus: Composition, Synthesis and Organization. Adv. Drug Delivery Rev. 2018, 124, 3– 15, DOI: 10.1016/j.addr.2017.09.023 .
22 Dash, S.; Das, S. K.; Samal, J.; Thatoi, H. N. Epidermal Mucus, a Major Determinant in Fish Health: a Review. Iran J. Vet. Res. 2018, 19, 72– 81.
23 Chen, G.; Yu, Y.; Wu, X.; Wang, G.; Ren, J.; Zhao, Y. Bioinspired Multifunctional Hybrid Hydrogel Promotes Wound Healing. Adv. Funct. Mater. 2018, 28, 1801386 DOI: 10.1002/adfm.201801386 .
24 Li, X.; Bai, H.; Yang, Y.; Yoon, J.; Wang, S.; Zhang, X. Supramolecular Antibacterial Materials for Combatting Antibiotic Resistance. Adv. Mater. 2018, 0, 1805092 DOI: 10.1002/adma.201805092 .
25 Hu, B.; Owh, C.; Chee, P. L.; Leow, W. R.; Liu, X.; Wu, Y.-L.; Guo, P.; Loh, X. J.; Chen, X. Supramolecular Hydrogels for Antimicrobial Therapy. Chem. Soc. Rev. 2018, 47, 6917– 6929, DOI: 10.1039/C8CS00128F .
2 6Ding, X.; Duan, S.; Ding, X.; Liu, R.; Xu, F.-J. Versatile Antibacterial Materials: An Emerging Arsenal for Combatting Bacterial Pathogens. Adv. Funct. Mater. 2018, 28, 1802140 DOI: 10.1002/adfm.201802140 .
27 Hu, B.; Shen, Y.; Adamcik, J.; Fischer, P.; Schneider, M.; Loessner, M. J.; Mezzenga, R. Polyphenol-Binding Amyloid Fibrils Self-Assemble into Reversible Hydrogels with Antibacterial Activity. ACS Nano 2018, 12, 3385– 3396, DOI: 10.1021/acsnano.7b08969 .
28 Irwansyah, I.; Li, Y.-Q.; Shi, W.; Qi, D.; Leow, W. R.; Tang, M. B. Y.; Li, S.; Chen, X. Gram-Positive Antimicrobial Activity of Amino Acid-Based Hydrogels. Adv. Mater. 2015, 27, 648– 654, DOI: 10.1002/adma.201403339 .
29 Gu, J.; Su, Y.; Liu, P.; Li, P.; Yang, P. An Environmentally Benign Antimicrobial Coating Based on a Protein Supramolecular Assembly. ACS Appl. Mater. Interfaces 2017, 9, 198– 210, DOI: 10.1021/acsami.6b13552 .
30 Wu, Y.; Wang, L.; Zhao, X.; Hou, S.; Guo, B.; Ma, P. X. Self-healing Supramolecular Bioelastomers with Shape Memory Property as a Multifunctional Platform for Biomedical Applications via Modular Assembly. Biomaterials 2016, 104, 18– 31, DOI: 10.1016/j.biomaterials.2016.07.011 .
31 Shang, L.; Zhang, W.; Xu, K.; Zhao, Y. Bio-inspired Intelligent Structural Color Materials. Mater. Horiz. 2019, 6, 945– 958, DOI: 10.1039/C9MH00101H .
32 Liu, K.; Liu, Y.; Yao, Y.; Yuan, H.; Wang, S.; Wang, Z.; Zhang, X. Supramolecular Photosensitizers with Enhanced Antibacterial Efficiency. Angew. Chem., Int. Ed. 2013, 52, 8285– 8289, DOI: 10.1002/anie.201303387 .
33 Bai, H.; Yuan, H.; Nie, C.; Wang, B.; Lv, F.; Liu, L.; Wang, S.; Supramolecular, A. Antibiotic Switch for Antibacterial Regulation. Angew. Chem., Int. Ed. 2015, 54, 13208– 13213, DOI: 10.1002/anie.201504566 .
34 Li, L.-L.; Xu, J.-H.; Qi, G.-B.; Zhao, X.; Yu, F.; Wang, H. Core–Shell Supramolecular Gelatin Nanoparticles for Adaptive and “On-Demand” Antibiotic Delivery. ACS Nano 2014, 8, 4975– 4983, DOI: 10.1021/nn501040h .
3 5Li, L.-L.; An, H.-W.; Peng, B.; Zheng, R.; Wang, H. Self-assembled Nanomaterials: Design Principles, the Nanostructural Effect, and Their Functional Mechanisms as Antimicrobial or Detection Agents. Mater. Horiz. 2019, 6, 1794– 1811, DOI: 10.1039/C8MH01670D .

36 Dong, S.; Leng, J.; Feng, Y.; Liu, M.; Stackhouse, C. J.; Schönhals, A.; Chiappisi, L.; Gao, L.; Chen, W.; Shang, J.; Jin, L.; Qi, Z.; Schalley, C. A. Structural Water as An Essential Comonomer in Supramolecular Polymerization. Sci. Adv. 2017, 3, eaao0900 DOI: 10.1126/sciadv.aao0900
3 7Zhang, Q.; Li, T.; Duan, A.; Dong, S.; Zhao, W.; Stang, P. J. Formation of a Supramolecular Polymeric Adhesive via Water–Participant Hydrogen Bond Formation. J. Am. Chem. Soc. 2019, 141, 8058– 8063, DOI: 10.1021/jacs.9b02677 .
38 Liu, M.; Liu, P.; Lu, G.; Xu, Z.; Yao, X. Multiphase-Assembly of Siloxane Oligomers with Improved Mechanical Strength and Water-Enhanced Healing. Angew. Chem., Int. Ed. 2018, 57, 11242– 11246, DOI: 10.1002/anie.201805206 .
39 Liu, M.; Wang, Z.; Liu, P.; Wang, Z.; Yao, H.; Yao, X. Supramolecular Silicone Coating Capable of Strong Substrate Bonding, Readily Damage Healing, and Easy Oil Sliding. Sci. Adv. 2019, 5, eaaw5643 DOI: 10.1126/sciadv.aaw5643
40 Yanagisawa, Y.; Nan, Y.; Okuro, K.; Aida, T. Mechanically Robust, Readily Repairable Polymers via Tailored Noncovalent Cross-linking. Science 2018, 359, 72– 76, DOI: 10.1126/science.aam7588 .
41 Zhang, J.; Liu, P.; Yi, B.; Wang, Z.; Huang, X.; Jiang, L.; Yao, X. Bio-Inspired Elastic Liquid-Infused Material for On-Demand Underwater Manipulation of Air Bubbles. ACS Nano 2019, 13, 10596– 10602, DOI: 10.1021/acsnano.9b04771 .
42 Gao, Y.; Wu, K.; Suo, Z. Photodetachable Adhesion. Adv. Mater. 2019, 31, 1806948 DOI: 10.1002/adma.201906193 .
43 Zhang, Q.; Shi, C.-Y.; Qu, D.-H.; Long, Y.-T.; Feringa, B. L.; Tian, H. Exploring a Naturally Tailored Small Molecule for Stretchable, Self-healing, and Adhesive Supramolecular Polymers. Sci. Adv. 2018, 4, eaat8192 DOI: 10.1126/sciadv.aat8192
44 Yi, B.; Liu, P.; Hou, C.; Cao, C.; Zhang, J.; Sun, H.; Yao, X. Dual-Cross-Linked Supramolecular Polysiloxanes for Mechanically Tunable, Damage-Healable and Oil-Repellent Polymeric Coatings. ACS Appl. Mater. Interfaces 2019, 11, 47382– 47389, DOI: 10.1021/acsami.9b17199 .
45 Jiang, J.; Gao, J.; Zhang, H.; He, W.; Zhang, J.; Daniel, D.; Yao, X. Directional Pumping of Water and Oil Microdroplets on Slippery Surface. Proc. Natl. Acad. Sci. U.S.A. 2019, 116, 2482– 2487, DOI: 10.1073/pnas.1817172116 .
46 DeVere, E.; Purchase, D. Effectiveness of Domestic Antibacterial Products in Decontaminating Food Contact Surfaces. Food Microbiol. 2007, 24, 425– 430, DOI: 10.1016/j.fm.2006.07.013 .
47 Zhang, D.; Leppäranta, O.; Munukka, E.; Ylänen, H.; Viljanen, M. K.; Eerola, E.; Hupa, M.; Hupa, L. Antibacterial Effects and Dissolution Behavior of Six Bioactive Glasses. J. Biomed. Mater. Res. Part A 2010, 93A, 475– 483
48 Gupta, A.; Mumtaz, S.; Li, C.-H.; Hussain, I.; Rotello, V. M. Combatting Antibiotic-resistant Bacteria Using Nanomaterials. Chem. Soc. Rev. 2019, 48, 415– 427, DOI: 10.1039/C7CS00748E .
49 Douglas, T. E. L.; Dziadek, M.; Schietse, J.; Boone, M.; Declercq, H. A.; Coenye, T.; Vanhoorne, V.; Vervaet, C.; Balcaen, L.; Buchweitz, M.; Vanhaecke, F.; Van Assche, F.; Cholewa-Kowalska, K.; Skirtach, A. G. Pectin-bioactive glass self-gelling, injectable composites with high antibacterial activity. Carbohydr. Polym. 2019, 205, 427– 436, DOI: 10.1016/j.carbpol.2018.10.061 .
50 Gupta, A.; Landis, R. F.; Li, C.-H.; Schnurr, M.; Das, R.; Lee, Y.-W.; Yazdani, M.; Liu, Y.; Kozlova, A.; Rotello, V. M. Engineered Polymer Nanoparticles with Unprecedented Antimicrobial Efficacy and Therapeutic Indices against Multidrug-Resistant Bacteria and Biofilms. J. Am. Chem. Soc. 2018, 140, 12137– 12143, DOI: 10.1021/jacs.8b06961 .

51 Magi, G.; Marini, E.; Facinelli, B. Antimicrobial Activity of Essential Oils and Carvacrol, and Synergy of Carvacrol and Erythromycin, against Clinical, Erythromycin-resistant Group A Streptococci. Front. Microbiol. 2015, 6, 165, DOI: 10.3389/fmicb.2015.00165 .
52 Chen, H.; Cheng, R.; Zhao, X.; Zhang, Y.; Tam, A.; Yan, Y.; Shen, H.; Zhang, Y. S.; Qi, J.; Feng, Y.; Liu, L.; Pan, G.; Cui, W.; Deng, L. An injectable Self-healing Coordinative Hydrogel with Antibacterial and Angiogenic Properties for Diabetic Skin Wound Repair. NPG Asia Mater. 2019, 11, 3 DOI: 10.1038/s41427-018-0103-9 .
53 van Doremalen, N.; Bushmaker, T.; Morris, D.; Holbrook, M.; Gamble, A.; Williamson, B.; Tamin, A.; Harcourt, J.; Thornburg, N.; Gerber, S.; Lloyd-Smith, J.; de Wit, E.; Munster, V. Aerosol and Surface Stability of HCoV-19 (SARS-CoV-2) Compared to SARS-CoV-1. New Engl. J. Med. 2020, DOI: 10.1056/NEJMc2004973 .
54 Xu, H.; Fang, Z.; Tian, W.; Wang, Y.; Ye, Q.; Zhang, L.; Cai, J. Green Fabrication of Amphiphilic Quaternized β-Chitin Derivatives with Excellent Biocompatibility and Antibacterial Activities for Wound Healing. Adv. Mater. 2018, 30, 1801100 DOI: 10.1002/adma.201801100 .
55 Zhao, X.; Li, P.; Guo, B.; Ma, P. X. Antibacterial and Conductive Injectable Hydrogels Based on Quaternized Chitosan-graft-polyaniline/oxidized Dextran for Tissue Engineering. Acta Biomater. 2015, 26, 236– 248, DOI: 10.1016/j.actbio.2015.08.006 .
56 Ben Arfa, A.; Combes, S.; Preziosi-Belloy, L.; Gontard, N.; Chalier, P. Antimicrobial Activity of Carvacrol Related to its Chemical Structure. Lett. Appl. Microbiol. 2006, 43, 149– 154, DOI: 10.1111/j.1472-765X.2006.01938.x